

Satellite-like CdS nanoparticles anchoring onto porous NiO nanoplates for enhanced visible-light photocatalytic properties

Hanmei Hu^{a,*}, Man Wang^a, Chonghai Deng^{b,c,*}, Jianli Chen^a, Aiguo Wang^a, Huirong Le^c

^a Key Laboratory of Functional Molecule Design and Interface Process, Anhui Jianzhu University, Hefei, 230601, China

^b Department of Chemical and Materials Engineering, Hefei University, Hefei, 230601, China

^c Department of Mechanical Engineering and Built Environment, University of Derby, Derby DE22 3AW, United Kingdom

* Corresponding author. *E-mail address*: hmhu@ustc.edu, chdeng@mail.ustc.edu.cn.

Abstract

Novel CdS/NiO nanocomposites assembled by satellite-like CdS nanoparticles anchoring onto porous NiO nanoplates have been fabricated by a step synthesis process, which involves a chemical bathing method followed by a heat treatment, and a microwave-assisted aqueous chemical reaction. The structure and photocatalytic properties of products were characterized by various techniques. More significantly, benefiting from the synergistic effect of CdS/NiO heterojunction, the as-prepared CdS/NiO architectures exhibited superior photocatalytic activity for decolorization of Congo red. The degradation rate on CdS/NiO nanocomposites achieves about 3.5 times higher than that of pure CdS nanocrystals under visible light irradiation for 30 min, suggesting a promising application in water purification.

Keywords: Semiconductors; CdS; NiO; nanocomposites; photocatalysis; water

purification

1. Introduction

The semiconductor-based photocatalysis technology is considered as an ecofriendly and efficient method of environmental remediation and solar fuel conversion [1, 2]. As an important semiconductor with a narrow and direct band gap, n-type CdS has been proven to be an excellent visible light photocatalyst in the field of water and air purification. Various CdS nanostructures have been fabricated by physicochemical methods for their practical applications in degradation of organic contaminants [3-5]. As is known, the photocatalytic reactions occur between the photoinduced activated radicals and the contaminant molecules on the interface. Compared with a monolithic photocatalyst, the nanocomposites composed of two or more semiconductors possess representative structures for photoelectrocatalytic applications with the merits of enhanced light adsorption, fast electron conducting, lower carrier recombination loss and shorter diffusion path for charge carriers [6, 7].

Also as a way of wastewater treatment for environmental remediation, p-type NiO semiconductor nanocrystals have shown the prominent adsorption behavior of anionic dye pollutants [8, 9]. Factually, enhancing adsorption of pollutant molecular on the surface of catalyst is a reliable strategy to improve the photoelectrocatalytic efficiency. More recently, some of NiO-based nanocomposites with improved photoatalytic performance have been developed, such as NiO/BiOX (X: Cl, I) and NiO/SiO₂ heterostructures [10-12]. However, to the best of our knowledge, the synthesis of CdS/NiO nanocomposites for synergistic enhancing adsorption and photocatalytic

properties has not been reported.

Herein, novel satellite-like CdS nanoparticles anchoring on porous NiO nanoplates were fabricated by a step synthesis process. The structure and composition of sample were characterized through various analysis methods. Thanks to the synergistic effect of CdS/NiO heterojunction, as-prepared CdS/NiO architecture exhibits excellent photodegradation efficiency for Congo red under visible light irradiation.

2. Experiment

All the chemicals were used as received without any further purification. Firstly, the porous NiO nanoplates were synthesized by a stepwise chemical bathing and followed by an annealing treatment. Then porous CdS/NiO nanocomposites were fabricated by a microwave-assisted aqueous chemical reaction, as illustrated in Fig.1. Briefly, the mixture solution containing 1mmol $\text{Ni}(\text{CH}_3\text{COO})_2 \cdot 4\text{H}_2\text{O}$ and 0.2-0.3 mL $\text{N}_2\text{H}_4 \cdot \text{H}_2\text{O}$ (85%) was transferred into a water bath at a temperature of 80 °C for 3 h, the blue plate-like precursor was collected. The precursor was annealed at 500 °C for 1 h in air to yield the porous NiO nanoplates. Subsequently, the suspension was fixed with 0.1g NiO nanoplates, 0.4 mmol $\text{Cd}(\text{CH}_3\text{COO})_2 \cdot 2\text{H}_2\text{O}$, 1 mmol thiourea (TU) and 0.1 mL ethylenediamine (en) under string continuously overnight, and then heated by microwave irradiation for 30 min, the CdS nanoparticles anchoring on NiO nanoplates with pores were finally constructed. The detailed preparation, characterization and photocatalytic performance measurements of sample are provided in **Supplementary information**. For comparison, pure CdS nanocrystals were obtained according to the same microwave heating reaction without adding NiO.

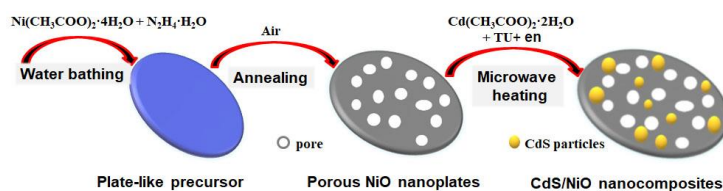


Fig.1. Schematic illustration of the synthesis of CdS/NiO nanocomposites

3. Results and Discussion

Fig.2a gives FESEM image of NiO products after annealing, which indicates that large quantities of the unique nanoplates have a diameter in range of 100~200 nm and the thicknesses of about 20 nm. Interestingly, lots of tiny irregular pores decorate on the surface of nanoplate, suggesting high porosity nature. The morphology of CdS/NiO nanocomposites is shown in Fig. 2b. It can be clearly seen that satellite-like CdS nanoparticles with sizes of 20-40 nm are tightly anchored onto the surface of porous NiO nanoplates, forming p-n heterostructures. It is fascinating to see that abundant mesopores still exist on the surface of crystals, but becoming smaller compared to pristine NiO nanoplates. Fig. 2c shows a high-resolution TEM image of CdS/NiO heterostructures. One can see that the crystal boundary between n-CdS and p-NiO is very clear, as depicted by the pink dotted line. The fringe spacing of 0.335 nm is correspond to (002) plane of hexagonal CdS, whereas the interplanar distance of 0.241 nm is in accordance with the lattice spacing of (111) plane of cubic NiO. The typical XRD pattern of composites is shown in Fig. 2d. All peaks in the diffraction diagram can be indexed to a hexagonal CdS (JCPDS 41-1049) and a cubic NiO (JCPDS 47-1049). No characteristic peaks of any impurities were detected. Further, the chemical compositions of the products were determined using a FESEM with

energy dispersive X-ray (EDX) analysis. As given in Fig 2e, the peaks of Cd, S, Ni and O elements are obviously observed, being consistence of the XRD result.

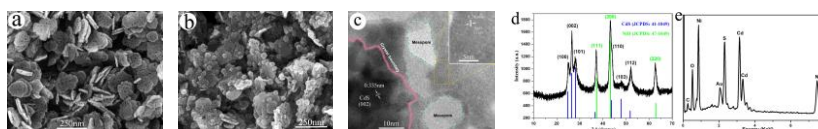


Fig.2. (a) FESEM image of NiO porous nanoplates, (b) FESEM and (c) HRTEM images, (d) XRD pattern and (e) EDX result of CdS/NiO nanocomposites

The N₂ adsorption-desorption isotherm and BET pore size distribution are depicted in Fig. 3a. The isotherm is identified as typical type IV pattern, indicating a hysteresis loop characteristic of mesoporesity. The BET specific surface area is measured to be 47.69 m²/g. From the corresponding pore diameter distribution curve (inset of Fig. 3a), the inhomogeneous mesoporous structures are observed and the multiple pore sizes are estimated to be 2.1, 8.1 and 34.3 nm in diameter, respectively. As given in Fig. 3b, the absorption band of pristine NiO nanoplates is located in ultraviolet region, whereas the absorption threshold of pure CdS and CdS/NiO composites is located at 585 and 600 nm, respectively, showing visible light absorption. Further, the optical absorption near the band gap was accordingly calculated using Tauc's formula [13], the values of E_g were estimated to be 3.29eV, 2.22eV and 2.31eV for NiO, CdS and CdS/NiO composite, respectively (inset of Fig.3b).

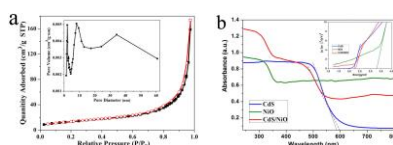


Fig. 3. (a) N₂ adsorption/desorption isotherms and pore size distribution (inset) and (b) UV-vis diffuse reflectance spectra (DRS) and E_g (inset) of CdS/NiO nanocomposites.

Congo red (CR) is an anionic secondary diazo dye. The decomposition of CR over CdS/NiO porous nanocomposites under visible light irradiation is displayed in Fig. 4a. The characteristic absorption peak of CR at around 497 nm undergo a fairly large decrease within 30 min. Fig.4b indicates the decolorization efficiency of CR over different catalysts. The dark adsorption rate on porous CdS/NiO nanocomposites goes up to 41.5%, which is about four times of that of CdS nanoparticles (10.6% only). As known, high adsorption is beneficial for enhancing catalytic reaction of photocatalyst. Not surprisingly, the CR degradation rate in the presence of pristine NiO almost unchanged under visible lighting, confirming that NiO is a good adsorbent of CR rather than a visible light photocatalyst. Besides, the direct photolysis of CR could be neglected in the blank experiment. Surprisingly, the degradation efficiency of CR over CdS/NiO nanocomposites achieves 92.1% under visible light irradiation for 30 min, showing about 3.5 times of that of pure CdS nanocrystals at 26.9%. As expected, as-prepared CdS/NiO nanocomposites exhibiting remarkable photocatalytic activity is attributed to the synergistic effect of CdS/NiO heterojunction. One reason is that CdS/NiO nanocomposites display the enhanced adsorption of CR on the surface of photocatalyst. More importantly, CdS/NiO heterojunctions promote the transfer of photogenerated e^-/h^+ pairs and hinder the recombination of charge carriers. Due to the conduction band (CB) of CdS (-0.88 eV, SHE) is more negative than that of NiO (0.0 eV, SHE) [14, 15], the electrons generated from CdS can promptly migrate from CB of CdS to that of NiO, meanwhile leaving the holes in valence band (VB) of CdS. Subsequently, the adsorbed O_2 can captured the electrons to produce superoxide

radical anions $\cdot\text{O}_2^-$, and the holes can react with OH^- to generate $\cdot\text{OH}$ radicals [16]. Further, those active radicals ($\cdot\text{O}_2^-$, h^+ and $\cdot\text{OH}$) can effectively mineralize CR into carbon dioxide and water. Thus the suggested photocatalytic degradation mechanism over CdS/NiO heterojunction is proposed in Fig.4c.

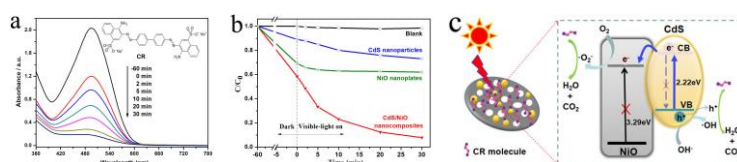


Fig.4. (a) Temporal absorption spectra of the solution of CR, (b) Photodegradation rate of CR and (c)

The proposed photocatalytic degradation mechanism on CdS/NiO heterojunction.

4. Conclusions

Novel porous CdS/NiO nanocomposites composed of CdS nanoparticles anchored on NiO nanoplates were constructed by a three-step process. As-prepared CdS/NiO architectures exhibited highly enhanced photodegradation of CR under visible light irradiation. The excellent photocatalytic property is attributed to the synergistic effect of CdS/NiO heterojunction, which not only enhance the adsorption of CR but also promote the transfer of charge carriers. This work may inspire energetic passion on the intensive study of other functional semiconductor heterostructures.

Acknowledgements

This work was supported by the Key Projects of Support Program for Outstanding Young Talents of Anhui Province (gxyqZD2016151), the Natural Science Foundation of Anhui Province (1808085MB40), the Program of Study Abroad for Excellent Young Scholar of Anhui Province (gxfxZD2016221), the Natural Science Foundation of Anhui Province Educational Committee (KJ2014ZD08, KJ2015A145), and the Special Foundation for Scientists of Hefei University (15CR06).

References

- [1] R. Asahi, T. Morikawa, T. Ohwaki, K. Aoki, Y. Taga, *Science* 293 (2001) 269-71.
- [2] Z. Zou, J. Ye, K. Sayama, H. Arakawa, *Nature* 414 (2001) 625-7.
- [3] C. Deng, X. Tian, *Materials Research Bulletin* 48 (2013) 4344-50.
- [4] Y. Xu, C. Song, Y. Sun, D. Wang, *Materials Letters* 65 (2011) 1762-4.
- [5] Z. Yu, X. Wu, J. Wang, W. Jia, G. Zhu, F. Qu, *Dalton Transactions* 42 (2013) 4633-8.
- [6] A. Arshad, J. Iqbal, M. Siddiq, M.U. Ali, A. Ali, H. Shabbir, U.B. Nazeer, M.S. Saleem, *Ceramics International* 43 (2017) 10654-60.
- [7] H. Jia, B. Zhang, W. He, Y. Xiang, Z. Zheng, *Nanoscale* 9 (2017) 3180-7.
- [8] H. Hu, G. Chen, C. Deng, Y. Qian, M. Wang, Q. Zheng, *Materials Letters* 170 (2016) 139-41.
- [9] H. Hu, M. Wang, H. Xuan, K. Zhang, J. Xu, *Micro & Nano Letters* 12 (2017) 987-90.
- [10] L. Yosefi, M. Haghghi, *Applied Catalysis B: Environmental* 220 (2018) 367-78.
- [11] X. Sun, Y. Zhang, P. Li, D. Guo, H. Zi, J. Guo, Y. Li, *Journal of Alloys and Compounds* (2017).
- [12] M.S. Akhtar, M.A. Alam, K. Tauer, M.S. Hossan, M.K. Sharafat, M.M. Rahman, H. Minami, H. Ahmad, *Colloids and Surfaces A: Physicochemical and Engineering Aspects* 529 (2017) 783-92.
- [13] J. Tauc, T.A. Scott, *Physics Today* 20 (1967) 105.
- [14] Y. Xu, M.A.A. Schoonen, *American Mineralogist* 85 (2000) 543-56.
- [15] A. Kudo, Y. Miseki, *Chemical Society Reviews* 38 (2009) 253-78.
- [16] S. Sakthivel, H. Kisch, *Angewandte Chemie International Edition* 42 (2003) 4908-11.